Available online at www.sciencedirect.com
SCIENCE DIRECT®
Journal of Power Sources 119–121 (2003) 733–737
JOURNAL OF POWER SOURCES
www.elsevier.com/locate/jpowsour

Relation between crystal structures, electronic structures, and electrode performances of $LiMn_{2-x}M_xO_4$ (M = Ni, Zn) as a cathode active material for 4V secondary Li batteries

Yuka Ito, Yasushi Idemoto*, Yuka Tsunoda, Nobuyuki Koura

Department of Pure and Applied Chemistry, Faculty of Science and Technology, Tokyo University of Science, 2641 Yamazaki, Noda, Chiba 278-8510, Japan

Abstract

We investigated the relation between the electrode performance and electronic states of $LiMn_{2-x}M_xO_4$ (M = Ni, Zn) as cathode active materials for the 4V class of lithium secondary batteries. The cycle performance is improved by substitution of Mn with Ni or Zn. We obtained the electron density distribution by XRD using the *MEM/Rietveld* method. Moreover, we investigated the electronic states of $LiMn_{1.75}M_{0.25}O_4$ (M = Mn, Ni, Zn) using first-principles calculation by the DV-Xα method. The net charges of each atom, and the bond overlap populations of Li–O, Mn–O, Ni–O and Zn–O were calculated. From the results, Li has a high ionicity and the covalent bonding of the Mn–O of $LiMn_{1.75}M_{0.25}O_4$ (M = Ni, Zn) is stronger than that of $LiMn_2O_4$. As a result of the DOS, the oxygen 2p orbital and Mn 3d orbital provides the overlap and the overlap of $LiMn_{1.75}M_{0.25}O_4$ is greater than that of $LiMn_2O_4$.

Keywords: Lithium manganese spinel; First-principles calculation; Substitution; MEM; Cathode active material; Electronic states

1. Introduction

$LiMn_2O_4$ is a well-known cathode material for 4V class lithium batteries. It has the advantages of low cost and low toxicity. However, its capacity loss during cycling in the 4V region has become an obstruction to practical use. The main factor of capacity loss is that Mn^{3+} dissolves during the cycling and produces an unstable spinel structure [1]. Recent work in order to improve the cycle performance is to substitute another transition metal of Mn with M, $LiMn_{2-x}M_xO_4$ (M = Li, Al, Ti, Ge, Fe, Co, Zn, Ni, Ga, Cu, Mg, Cr) [2–6].

In this study, we investigated the relation between the properties, the crystal structures, and electrode performances of $LiMn_{2-x}M_xO_4$ (M = Mn, Ni, Zn). We also estimated the ionicity, the bond overlap population (BOP), and the density of states of these materials using the first-principles calculation by the DV-Xα method.

2. Experimental

The $LiMn_{2-x}M_xO_4$ powders (M = Zn: $x = 0$, 0.05, 0.1; M = Ni: $x = 0$, 0.1, 0.3) were prepared by using $^7Li_2CO_3$, MnO_2, $Zn(NO_3)_2$ and $Ni(OH)_2$ so as to avoid the high neutron absorption of ^6Li. The mixtures were preheated at 600 °C for 24 h in air, then heated at 700–800 °C for 24 h in oxygen.

The samples were determined to be single phase and the evaluation of the lattice parameter was examined by XRD. The sample compositions were determined by ICP. The Mn valence was determined by iodometry, chelatometry and ICP [7].

The crystal structures were obtained from a Rietveld analysis (Rietan 2000) by neutron powder diffractions using the HERMES [8] of IMR at JPR-3M. From the results, we calculated the bond length of Mn, Zn, Ni (16d)–O (32e), Li (8a)–O (32e). We also calculated the Madelung energy using the Rietveld analysis results. The electron density distributions of $LiMn_{2-x}M_xO_4$ (M = Mn, Ni, Zn) were analyzed by the *MEM/Rietveld* method using the XRD results.

The electrochemical measurement used a three-electrode cell. The cell consisted of the $LiMn_{2-x}M_xO_4$ (M = Ni: $x = 0$, 0.1, 0.3; M = Zn: $x = 0$, 0.05, 0.1) cathode (WE) and Li films (CE and RE). The cathode was prepared by pressing a blend of active material (25 mg), acetylene black (10 mg) and PTFE (10 mg) onto a Ni mesh and then drying at 150 °C for 12 h under vacuum. The electrolyte used was a 1 M $LiClO_4$–PC/DMC (1:1) solution. All procedures were carried out in an argon-filled glove box.

* Corresponding author. Tel.: +81-4-7124-1501; fax: +81-4-7125-7761.
E-mail address: idemoto@rs.noda.tus.ac.jp (Y. Idemoto).

0378-7753/03/$ – see front matter © 2003 Elsevier Science B.V. All rights reserved.
doi:10.1016/S0378-7753(03)00212-X

The charge–discharge tests were performed at a constant current density (0.2 mA cm^{-2}) with cut-off potentials of 3.5–4.3 V versus Li/Li^+ at 25 and 50 °C.

We investigated the ionicity and the covalency of the atoms for $LiMn_{2-x}M_xO_4$ (M = Ni, Zn, Mn) using a first-principles calculation. We examined the net charges, the bond overlap populations, and the density of states by the discrete variational DV-Xα method on model clusters.

3. Results and discussion

3.1. Sample characterization

The powder X-ray diffraction profiles of the $LiMn_{2-x}M_xO_4$ (M = Ni: $x = 0$, 0.1, 0.3; M = Zn: $x = 0$, 0.05, 0.1) were identified as a single phase cubic spinel with the space group $Fd\bar{3}m$. The metal composition of these samples, which were determined by ICP, are the same as the nominal composition. Next, the Mn valence was determined by iodometory, chelatometry and ICP. Fig. 1 shows the relation between the Mn valence and lattice parameter, a, determined by the XRD of $LiMn_{2-x}M_xO_4$ (M = Zn, Ni). The Mn valence increases and the lattice parameter a decreased with the increasing Ni or Zn content. From these results, the substitution of Ni^{3+} or Zn^{2+} into the Mn-site is accompanied by the oxidation of Mn^{3+} to Mn^{4+}.

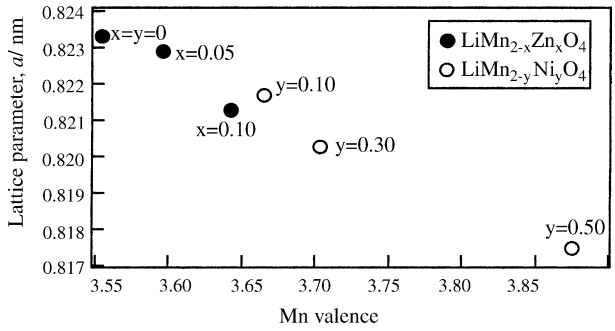

Fig. 1. Relationship between Mn valence and lattice parameter determined by X-ray diffraction measurement of $LiMn_{2-x}Zn_xO_4$ and $LiMn_{2-y}Ni_yO_4$.

Table 1
Final results of the Rietveld refinements for $^7LiMn_{1.95}Zn_{0.05}O_4$ in space group $Fd\bar{3}m$ (Cubic, $z = 4$)

Atom	Site	x	y	z	B (nm^2)
Li	8a	0	0	0	0.0107 (19)
Mn, Zn	16d	5/8	5/8	5/8	0.0028 (6)
O	32e	0.38818 (8)	0.38818 (8)	0.38818 (8)	0.0089 (4)

B are isotropic thermal parameters. The site Mn, Zn is occupied by Mn and Zn in a 0.975:0.025 ratio. The sites Li and O are occupied fully. Numbers in parentheses are estimated standard deviations of the last significant digit, and those without deviations were fixed. R_{wp}: 6.84%, R_e: 4.63%, R_p: 5.30%, S: 1.48, $a = 0.82308$ (7) nm, $V = 0.5576$ (1) nm^3.

3.2. Structural analysis of neutron powder diffraction data

The neutron-diffraction intensity profiles of $LiMn_{2-x}M_xO_4$ (M = Ni: $x = 0$, 0.1, 0.3; M = Zn: $x = 0$, 0.05, 0.1) were analyzed over a wide range at room temperature and 200 K. A refinement was carried out by assuming a cubic unit cell (space group $Fd\bar{3}m$) using Rietan 2000 [9]. The final results for $^7LiMn_{1.95}Zn_{0.05}O_4$ at room temperature are listed in Table 1. Fig. 2 shows the results of the refinement pattern for $LiMn_{1.95}Zn_{0.05}O_4$ at room temperature, where good agreement between the observed and calculated patterns were obtained. The results for the other materials show the same tendency. From these results at room temperature and 200 K, it is seen that the phase transition (cubic to orthorhombic) was restrained by substitution of M for Mn. The bond lengths of Li–O, (Mn, M)–O (M = Ni, Zn) and the Madelung energy decrease with the increasing M content. The bond lengths of the (Mn, M)–O dependence on temperature decreased with the increasing M content, x

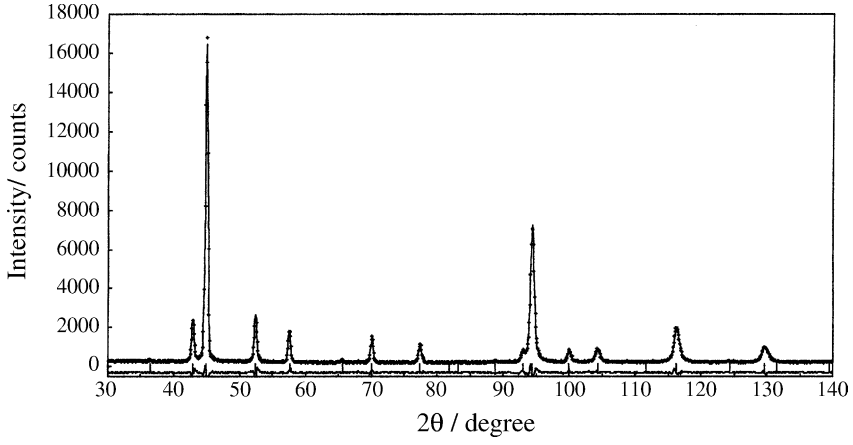

Fig. 2. Rietveld refinement patterns for $^7LiMn_{1.95}Zn_{0.05}O_4$. Plus marks show observed neutron diffraction intensities, and a solid line represents calculated intensities. The vertical marks below the patterns indicate the positions of allowed Bragg reflections. The curve at the bottom is the difference between the observed and calculated intensities in the same scale.

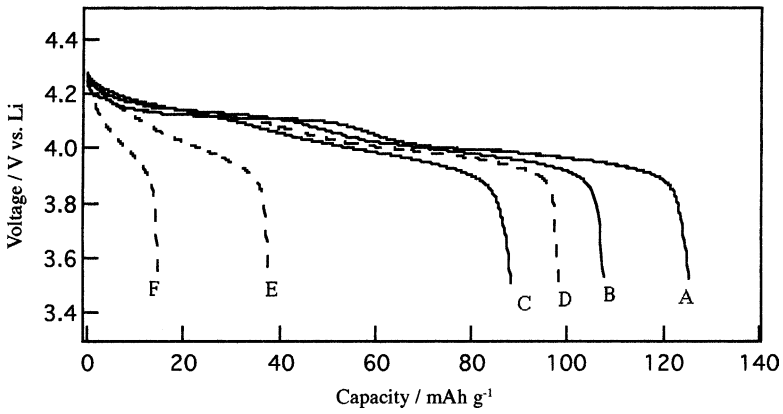

Fig. 3. Galvanostatic discharge curves for the first cycle of LilLiMn$_{2-x}$M$_x$O$_4$ (M = Ni, Zn) cells at 25 °C and 0.2 mA cm^{-2}. A: $x = 0$, B: M = Zn; $x = 0.05$, C: M = Zn; $x = 0.10$, D: M = Ni; $x = 0.1$, E: M = Ni; $x = 0.3$, F: M = Ni; $x = 0.5$.

(M = Zn, Ni). Hence, the crystal structure is made more stable by the substitution of Zn or Ni for Mn.

3.3. Evaluation of the electrode performance

Fig. 3 shows the galvanostatic discharge curves for the LilLiMn$_{2-x}$M$_x$O$_4$ (M = Ni, Zn) cells during the first cycle at 25 °C. The first discharge capacity decreases with increasing M content since the Mn valence increases with the increasing M content. The discharge capacity in the 4V region is very low for LiMn$_{1.5}$Ni$_{0.5}$O$_4$ since the Mn valence is almost 4. The material was used for the 5V class cathode active materials [10]. The two plateaus are less distinct with the increasing M content. This suggests that the single phase region of LiMn$_{2-x}$M$_x$O$_4$ (M = Ni, Zn) is maintained during the charge–discharge with an increasing M content. Table 2 shows the capacity of the first cycle and the fade in the discharge capacity after the first discharge for various LiMn$_{2-x}$M$_x$O$_4$ (M = Ni, Zn) compounds at 25 and 50 °C. From these results, it can be seen that a significant improvement in the cycle performance was observed with an increase in the Ni or Zn content. The cycling performance at 50 °C has the same trend as that at room temperature. These results are similar when substituting a part of Mn with Li or Mg [6,7,11].

3.4. Investigation of electronic structure by first-principles calculation

For the theoretical investigation of the structural stability and bonding state as a function of substitution of Mn with Zn or Ni, the ionicity was estimated from the net charge of

Table 2
The capacity of first cycle and the fade of discharge capacity for the first discharge capacity of LiMn$_{2-x}$M$_x$O$_4$ (M = Ni, Zn) at 0.2 mA cm^{-2} and 25, 50 °C

Sample	Capacity of first cycle (mAh g^{-1})	10 cycles (%)	20 cycles (%)	30 cycles (%)	40 cycles (%)	50 cycles (%)
(a) LiMn$_{2-x}$Zn$_x$O$_4$ at 25 °C						
$x = 0$	125.6	90.8	80.6	71.1	64.1	57.9
$x = 0.05$	107.4	96.0	92.9	71.1	70.1	58.8
$x = 0.1$	88.2	99.0	98.9	98.4	97.8	97.2
(b) LiMn$_{2-x}$Ni$_x$O$_4$ at 25 °C						
$x = 0$	125.6	90.8	80.6	71.1	64.1	57.9
$x = 0.1$	92.4	92.9	85.0	77.2	69.3	61.4
$x = 0.3$	37.8	98.1	97.4	97.0	96.1	96.1
$x = 0.5$	15.0	100	100	99.2	98.6	97.9
(c) LiMn$_{2-x}$Zn$_x$O$_4$ at 50 °C						
$x = 0$	124.5	76.7	59.0	48.2	41.0	35.1
$x = 0.05$	101.4	93.1	82.5	71.8	61.9	52.8
$x = 0.10$	82.4	93.4	86.2	78.9	–	–
(d) LiMn$_{2-x}$Ni$_x$O$_4$ at 50 °C						
$x = 0$	124.5	76.7	59.0	48.2	41.0	35.1
$x = 0.1$	80.3	92.9	85.0	77.2	69.3	61.4
$x = 0.3$	39.9	91.3	90.1	90.0	87.9	86.1
$x = 0.5$	15.4	98.4	98.4	98.2	97.9	97.3

Table 3
Results of bond overlap population of atoms for $LiMn_{1.75}M_{0.25}O_4$

M	Mn–O	M–O	Li–O
Mn	0.203	0.237	0.019
Zn	0.266	0.137	0.014
Ni	0.211	0.219	0.013

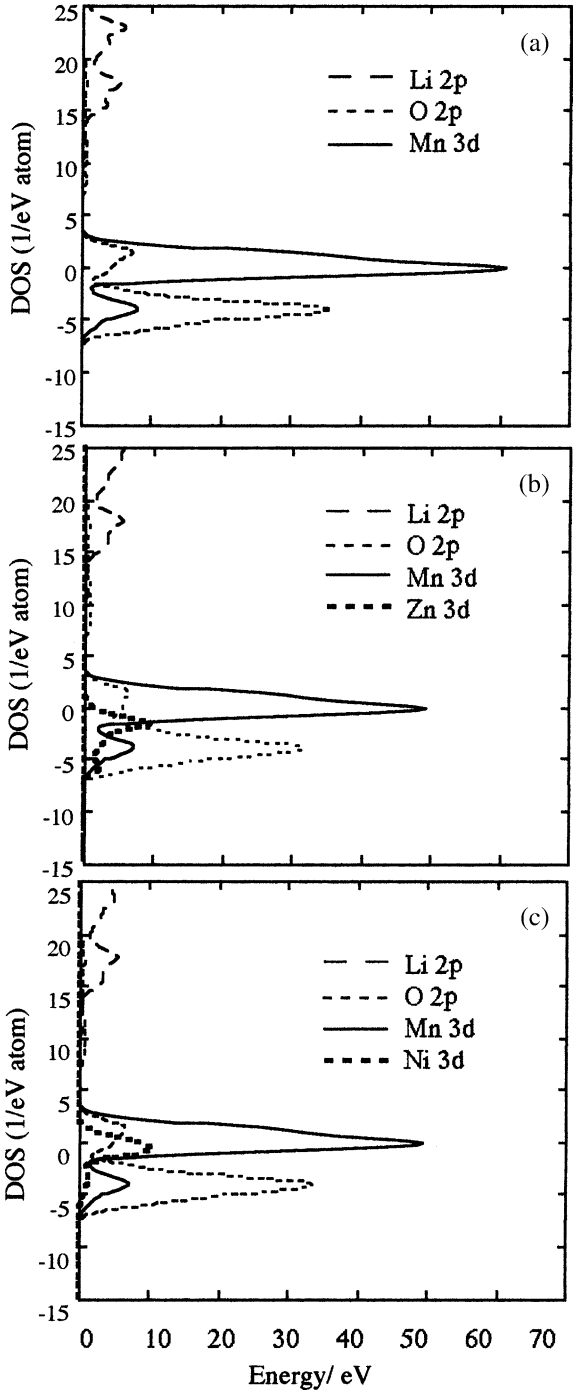

Fig. 4. Density of states for $LiMn_{1.75}M_{0.25}O_4$ cluster. Broken line shows Li 2p, a dotted line shows O 2p orbital, a bold dotted line shows M (M = Zn, Ni) 3d orbital, and a solid line shows Mn 3d orbital. (a) M = Mn; (b) M = Zn; (c) M = Ni.

atoms and the covalency was estimated from the bond overlap population of each atom using first-principles calculations by the DV-Xα method. From the net charge results, the Li is shown to have a high ionicity in all cases [12]. The ionicity of Zn and Ni is slightly lower than that of Mn. Table 3 shows the bond overlap population (BOP) for $LiMn_{1.75}M_{0.25}O_4$ (M = Mn, Zn, Ni). The BOP of Mn–O increases with the substitution of Mn with M (Zn, Ni). On the other hand, the BOP of Li–O is low, that is it corresponds with the high ionicity of Li. The BOP of Mn–O, which holds for most of the 16d sites, for $LiMn_{1.75}M_{0.25}O_4$ (M = Ni, Zn) is stronger than that of $LiMn_2O_4$.

The electron density distributions of $LiMn_{1.75}M_{0.25}O_4$ (M = Mn, Ni, Zn) were also calculated using first-principles by the DV-Xα method. Fig. 4 shows the densities of states for $LiMn_{1.75}M_{0.25}O_4$ (M = Mn, Ni, Zn). The O 2p orbital and Mn 3d orbital provide the overlap. The overlap of $LiMn_{1.75}Zn_{0.25}O_4$ is greater than that of $LiMn_2O_4$. Hence, the Li ionicity remains high and strong covalent bonding of Mn–O was found for substitution of part of the Mn with Zn. There is the same tendency for $LiMn_{1.75}Ni_{0.25}O_4$, but the difference is small compared to $LiMn_2O_4$. Consequently, the crystal structure is made more stable by substitution of part of the Mn with Zn or Ni.

4. Conclusion

The cycling performance was improved with increasing Zn or Ni content (x in $LiMn_{2-x}M_xO_4$). The phase transition was restrained by the substitution of Zn and Ni for Mn. From the first-principles calculation, the Li ionicity remained high and the Mn–O covalent bonding for the substitution of Mn with M (M = Zn, Ni) is stronger than that of $LiMn_2O_4$. Hence, the crystal structure is made more stable by the substitution of Mn with Ni or Zn. Consequently, the cycling performance closely correlates with the structural stability.

Acknowledgements

We were indebted to Dr. A. Toubou, Dr. K. Ooyama, and Prof. Y. Yamaguchi (Tohoku University) for measurement of powder neutron diffraction at HERMES (IMR at JPR-3M).

References

[1] R.J. Gummow, A. de Kock, M.M. Thackeray, J. Solid State Ionics 69 (1994) 59.
[2] J.M. Tarascon, E. Wang, F.K. Shokoohi, W.M. McKinnon, S. Colson, J. Electrochem. Soc. 138 (1991) 2859.
[3] Q. Zhong, A. Banakdarpour, M. Zhang, Y. Gao, J.R. Dahn, J. Electrochem. Soc. 144 (1997) 205.
[4] L. Gouhara, H. Ikuta, T. Uchida, M. Wakihara, J. Electrochem. Soc. 143 (1996) 178.
[5] Y. Ein-Eli, W.F. Howard Jr., J. Electrochem. Soc. 144 (1997) L205.

[6] Y. Idemoto, S. Ogawa, Y. Uemura, N. Koura, J. Ceram. Soc. Jpn. 108 (2000) 848.
[7] Y. Idemoto, N. Koura, K. Udagawa, Electrochemistry (Denki Kagaku) 67 (1999) 235.
[8] K. Ohoyama, T. Kanouchi, K. Nemoto, M. Ohashi, T. Kajitani, Y. Yamaguchi, Jpn. J. Appl. Phys. 37 (1998) 3319.
[9] F. Izumi, T. Ikeda, Master. Sci. Forum 321 (2000) 198.
[10] Y. Idemoto, H. Narai, N. Koura, Electrochemistry 70 (2002) 587.
[11] Y. Idemoto, S. Ogawa, N. Koura, K. Udagawa, Electrochemistry 68 (2000) 469.
[12] Y. Ito, Y. Idemoto, N. Koura, Y. Tsunoda, Electrochemistry 70 (2002) 847.